



**HAL**  
open science

# FIRN DENSIFICATION BY GRAIN-BOUNDARY SLIDING : A FIRST MODEL

R. Alley

► **To cite this version:**

R. Alley. FIRN DENSIFICATION BY GRAIN-BOUNDARY SLIDING : A FIRST MODEL. Journal de Physique Colloques, 1987, 48 (C1), pp.C1-249-C1-256. 10.1051/jphyscol:1987135 . jpa-00226281

**HAL Id: jpa-00226281**

**<https://hal.science/jpa-00226281>**

Submitted on 4 Feb 2008

**HAL** is a multi-disciplinary open access archive for the deposit and dissemination of scientific research documents, whether they are published or not. The documents may come from teaching and research institutions in France or abroad, or from public or private research centers.

L'archive ouverte pluridisciplinaire **HAL**, est destinée au dépôt et à la diffusion de documents scientifiques de niveau recherche, publiés ou non, émanant des établissements d'enseignement et de recherche français ou étrangers, des laboratoires publics ou privés.

## FIRM DENSIFICATION BY GRAIN-BOUNDARY SLIDING : A FIRST MODEL

R.B. ALLEY

*Geophysical and Polar Research Center, University of Wisconsin-Madison, 1215 W. Dayton Street, Madison, WI 53706, U.S.A.*

**Résumé** - La densification de névés très poreux à température constante se produit d'abord par glissement Newtonien sur les joints de grains, mais le nombre de coordination croît avec la densité et limite le glissement ultérieur. Pour une densité relative d'environ 0,6 le nombre de coordination est de l'ordre de 6 et le glissement n'est plus alors le mécanisme principal de densification ; la diminution de la vitesse de densification conduit à l'observation d'un point critique dans les profils densité/profondeur. Un modèle simple pour la densification par glissement aux joints conduit à une bonne correspondance avec les profils observés. La viscosité ainsi obtenue donne une énergie d'activation égale à celle de la diffusion des joints de grains.

**Abstract.** Densification in highly porous, isothermal firn occurs primarily by Newtonian sliding on grain boundaries, but the coordination number increases with density and restricts further sliding. At a relative density of about 0.6 the coordination number approaches 6 and sliding ceases to be a primary mechanism of densification; the resulting decrease in densification rate causes the critical point in depth-density profiles. A simple model for densification by boundary sliding yields a good fit to observed profiles. The viscosities so obtained give an activation energy equal to that for grain-boundary diffusion.

### I. Introduction

Densification in polar firn is analogous to pressure sintering in engineering practice [1]. At relative densities (= volume fraction of ice) above 0.6 to 0.7 sintering theories for pore shrinkage by center-to-center approach of grains provide a good fit to observations [2, 3] although the fit is not perfect [4]. However, at lower densities the observed densification rate exceeds that predicted by sintering theories by more than an order of magnitude [2, 3, this study].

Anderson and Benson [5] observed that highly porous firn densifies rapidly but that the densification rate decreases sharply at a "critical point" of relative density 0.6. Because this density corresponds to the random-closest-packing density for monosized spheres, Anderson and Benson speculated that rearrangement of unbonded grains dominates densification in highly porous firn and ceases at the critical point. However, Gow [1] showed that bonding in natural firn is well developed even at shallow depths so that simple rearrangement of unbonded grains cannot be important; nonetheless, it has been evident that grain rearrangement contributes to densification of highly porous firn in some manner [e.g. 3].

Grain-boundary-sliding theory [6] suggests that material deformation is dominated by linear-viscous boundary sliding at stresses less than  $10^{-4} G$ , where  $G$  is the shear modulus of the material; at higher stresses creep within grains dominates. Natural, highly porous firn falls within this range ( $G \approx 3.5 \times 10^9$  Pa [7], and stresses across bonds in firn are typically  $10^4$ - $10^5$  Pa [8]), although creep begins to be significant near the critical density. We thus expect that densification in highly porous firn is dominated by viscous boundary sliding. (As discussed below, a detailed calculation of densification by power-law creep across intergranular necks and by center-to-center approach of grains through boundary diffusion, lat-

tice diffusion, and power-law creep shows that these mechanisms cannot account for observed densification rates and suggests that we must consider boundary sliding.) Below we develop a simple model for firn densification by boundary sliding. We find that the model fits observed depth-density profiles well, and that the viscosities derived are reasonable and yield the expected activation energy.

II. Model

Firn densifies by vertical motion of grains (horizontal area is conserved). A grain subject to a vertical load will slide downward across grain bonds and cause densification if not constrained geometrically. Grain bonds in firn are large (bond radius: grain radius  $\approx 0.6-0.7$  below 10 cm depth [9], so bonds are distributed over the surface of a grain. A grain supported by a tripod of bonds (coordination number  $N \approx 6$ ) will not be free to move, whereas a grain supported by only two neighbors ( $N \approx 4$ ) will slide. Thus, as  $N$  increases from 4 to 6, sliding should cease to be a primary mechanism of densification [10]. (Geometric changes caused by other sintering mechanisms at higher densities can allow localized sliding, of course.) We observe that  $N$  approaches 6 at the critical density of 0.6 (Fig. 1).

To model the geometric freedom of grains first consider Figure 2, in which two spherical grains are connected across a bond centered at spherical coordinates  $(\theta, \phi)$  relative to the center of the upper grain ( $N \approx 2$ ). (We use "grain" to mean both a geometrically distinct particle and a monocrystal because most geometrically distinct particles are monocrystals in the depth range of interest here [11].) A vertical force,  $F_z$ , applied to the upper grain will cause a shear force  $F_s = F_z \sin \theta$  across the bond. (The assumption of vertical force is discussed with other assumptions below.) For a linear-viscous grain bond of thickness  $\lambda$ , viscosity  $\nu$ , and area  $A$ , the sliding velocity,  $u_s$ , will be

$$u_s = \frac{\lambda}{\nu} \frac{F_s}{A} \tag{1}$$

The vertical sliding velocity is  $u_z = u_s \sin \theta$ . If bonds are distributed randomly over grains, then the spherical average of  $u_z$  taken over many grains,  $\bar{u}_z$ , is given by

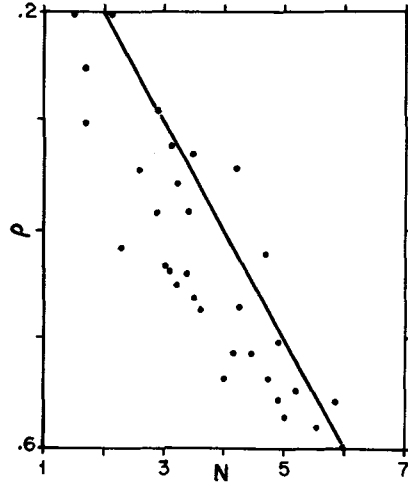


Fig. 1. Relative density ( $\rho$ ) vs. coordination number ( $N$ ) for firn from ridge BC and upstream B, West Antarctica, and from site A, Greenland. The approximation  $N = 10\rho$  also is shown. Use of an approximation that fits the data better would complicate the rate equations without changing them significantly.

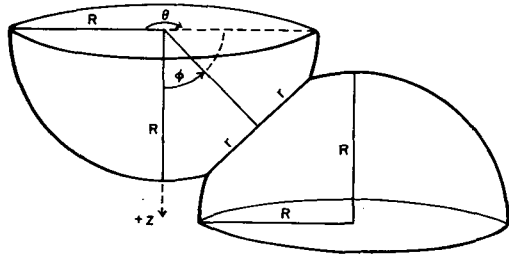


Fig. 2. Geometry of grains and bonds used in model. Variables are defined in text.

$$\bar{u}_z = \int_0^{\pi/2} u_z \sin\theta d\theta = \frac{\lambda}{v} \frac{F_z}{A} \int_0^{\pi/2} \sin^3\theta d\theta \equiv \frac{\lambda}{v} \frac{F_z}{A} \alpha' \quad (2)$$

where the geometric term  $\alpha'(N=2) = 2/3$ .

Now consider two bonds in the lower hemisphere ( $N \approx 4$ ). The bonds have normals  $A = (\theta_1, \phi_1)$ , and  $B = (\theta_2, \phi_2)$ . Sliding occurs in the plane of both bonds, and thus in the direction of  $A \times B$ . We call the downward component of this direction  $\phi_3$  (or  $\cos\phi_3$ ). From the usual transformation of spherical to rectangular coordinates in which the  $+z$  axis is  $\phi = 0$ ,  $\cos\phi_3$  is simply the  $+z$  coordinate of the unit vector in the direction of  $A \times B$ , taken in the positive direction.

The vertical sliding velocity is  $u_z = u_s \cos\phi_3$ , and the force causing shearing is  $F_s = F_z \cos\phi_3$ . Then  $\bar{u}_z$  is given by Equation (2), but the geometric term  $\alpha'(N=4)$  is the spherical average of  $\cos^2\phi_3$ , which in turn requires averaging over all  $(\theta_1, \phi_1)$  and  $(\theta_2, \phi_2)$ . We have calculated  $\alpha'(N=4)$  using a Monte Carlo simulation. We find that  $\alpha'(N=4) = 0.308$  for infinitesimal bonds. Real bonds have radii,  $r$ , equal to 0.6-0.7 of grain radii,  $R$  [9]. If we require that bond centers be at least  $1.2R$  apart in space, so that bonds do not overlap, then  $\alpha'(N=4) = 0.324$ .

The vertical velocity from Equation (2) can be used to calculate the densification rate. From Figure 2, the height of a cell,  $z = 2R \cos\phi$ , is the distance between grain centers. The average cell height,  $\bar{z}$ , is  $z$  averaged over  $\phi$  for all pairs of grains, which is simply  $\bar{z} = R$ . The average relative rate of densification then is

$$\frac{\dot{\rho}}{\rho} = \frac{\bar{u}_z}{\bar{z}} = \frac{\bar{u}_z}{R} \quad (3)$$

where  $\rho$  is the relative density and  $\dot{\rho}$  is its time derivative.

It remains to calculate  $F_z$ , the average vertical force on a grain. Many stress-intensity factors have been proposed to correct for the effect of porosity on isotropic stress [e.g. 12, 8, 3]; here we derive a specific expression assuming that the stress on a grain is vertical (this assumption is discussed below).

A horizontal section through firm shows ice fraction  $\rho$ , with  $n'$  grains per unit area. If all grains are spherical with radius  $R$ , then the average grain as seen on the section plane has area  $2\pi R^2/3$ , and  $n' = 3\rho/(2\pi R^2)$ . The average stress in the ice is  $P/\rho$ , where  $P$  is the overburden pressure. Then the average force per grain,  $F_z$ , is

$$F_z = \frac{P}{\rho n'} = \frac{2\pi R^2 P}{3\rho^2} \quad (4)$$

The overburden pressure is  $P = \dot{b}gt$ , where  $\dot{b}$  is the mass accumulation rate,  $g$  is the acceleration of gravity, and  $t$  is the time since deposition of the sample under consideration.

We next need expressions for  $\alpha'$ ,  $N$ , and  $A$ . The bond area over which shearing occurs is approximately  $A = \pi r^2 N/2$  where  $r$  is the bond radius and the lower half of the grain has  $N/2$  bonds. If the geometric factor  $\alpha'$  varies smoothly with  $N$ , then a reasonable expression based on the calculations above is  $\alpha' = 1 - N/6$ . From Figure 1, the data are described well by  $N = 10\rho$ . We now can substitute these relations and Equations (1), (2), and (4) into Equation (3) to obtain the densification relation for linear-viscous boundary sliding:

$$\frac{\dot{\rho}}{\rho} = \frac{2}{15} \dot{b}g \frac{\lambda}{v} \frac{R}{r^2} \frac{1}{\rho^3} \left(1 - \frac{5}{3}\rho\right)t \quad (5)$$

The quantities,  $\dot{b}$ ,  $g$ ,  $\lambda$ , and  $\nu$  are constants at any site assuming isothermal conditions, and  $r$  and  $R$  vary only slowly, so Equation (5) shows that the densification rate increases linearly with time but decreases more rapidly with density.

(We also have conducted this derivation [to be published elsewhere] for densification by power-law creep across intergranular necks of thickness  $2q$ , assuming that the normal pressure across grain bonds arising from  $F_z$  is deviatoric and so contributes to the effective stress, and that the creep exponent is 3. The result is that

$$\frac{\dot{\rho}}{\rho} = \frac{2q}{R} A' \left( \frac{2R^2 \dot{b} g t}{15 r^2 \rho^3} \right)^3 \quad (1.8 - 3\rho) \quad (6)$$

where  $A'$  is the usual prefactor for creep. Our calculations indicate that this process is not significant at the stresses in natural firn, although it could become significant under applied loads in engineering or laboratory situations.)

III. Model Results

We have modeled densification in firn using data from Dome C, East Antarctica ( $-54.3^\circ\text{C}$ ,  $\dot{b} = 34 \text{ kg/m}^2/\text{a}$  [8]), South Pole ( $-51^\circ\text{C}$ ,  $70 \text{ kg/m}^2/\text{a}$  [11]), Ridge BC on the Siple Coast of West Antarctica ( $-26.5^\circ\text{C}$ ,  $83 \text{ kg/m}^2/\text{a}$ ), and Site A, near Crête, Greenland ( $-29.5^\circ\text{C}$ ,  $284 \text{ kg/m}^2/\text{a}$ ). Our model uses the rate equations for sintering from Maeno and Ebinuma [3], modified slightly to avoid the assumption of small necks and to allow for overburden pressure with the stress-concentration factor of Alley et al. [8]; the model also allows grain rearrangement by linear-viscous boundary sliding and by power-law creep (Equations (5) and (6)). Each numerical experiment was started at 2 m depth, the shallowest depth where temperature-gradient effects become unimportant [9]. For a numerical experiment we calculate the densification rate during a time step and thus the density at the end of the time step, and calculate the burial depth at the end of the time step from the new density and the mass-accumulation rate; grain size is adjusted at the end of each time step to reflect the observed grain-growth rate. All parameters in the model are known physical constants or measured quantities except the grain-boundary viscosity,  $\nu$ , so we choose  $\nu$  to give the best fit between observed and modeled depth-density profiles.

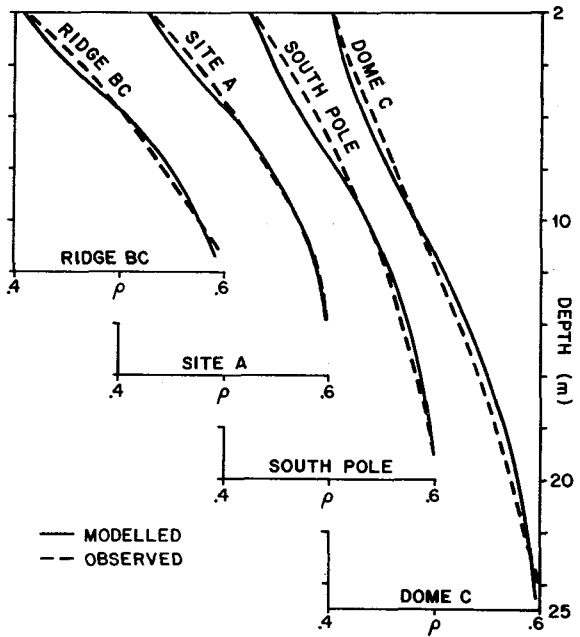


Fig. 3. Observed and modeled depth-density profiles for site A, Greenland and for ridge BC, South Pole, and Dome C, Antarctica.

The modeled depth-density profiles are compared to observations in Figure 3. The best-fit viscosities are plotted in Figure 4, and are: site A,  $\nu = 3 \times 10^7 \text{ Pa s}$ ; ridge BC,  $\nu = 6 \times 10^7 \text{ Pa s}$ ; South Pole,  $\nu = 2.5 \times 10^8 \text{ Pa s}$ ; Dome C,  $\nu = 7 \times 10^8 \text{ Pa s}$ . Errors in calculated viscosity arise from errors in matching observed and modeled profiles, from errors in model parameters (e.g.  $\dot{b}$ ,  $r$ ,  $R$ ), and from errors in the model itself. The error bars plotted in Figure 4 are about 22% of  $\nu$ , and represent the combined effects of estimated errors of 10% on  $\dot{b}$ ,  $r$ , and  $R$  plus a 10% error in matching observed and

modeled curves; errors in the model would increase the error bars further. The regression line in Figure 4 yields an activation energy for  $\nu$  of  $41 \pm 2$  kJ/mole.

#### IV. Discussion and Conclusions

Derivation of the model required several assumptions, including isotropy of bonds and vertical force on grains. Grain bonds in shallow firn actually show a preferred horizontal orientation, but become more isotropic with depth [9]. The stress state in firn is not known. It is probable that vertical forces dominate in the depth region of interest here, but the stress state probably becomes more hydrostatic with increasing depth [13]. These and other factors (including the effects of distributions of sizes and shapes of grains and bonds) should appear in a complete model of densification; however, we believe that their effects are small and will not change the model or results significantly.

The discussion by Ashby [14] shows that the viscosity of perfectly planar grain boundaries should approach that of supercooled liquid; however, real grain boundaries include roughness elements, such as ledges, inclusions, and other features. Raj and Ashby [15] have modeled grain-boundary sliding as controlled by molecular diffusion around obstacles through the grain boundary, giving the boundary viscosity as

$$\nu = \frac{kTh^2}{8D_b\Omega} \quad (7)$$

where  $k$  is Boltzmann's constant,  $T$  is absolute temperature,  $h$  is the amplitude of roughness elements,  $D_b$  is the grain-boundary diffusivity, and  $\Omega$  is the molecular volume. The activation energy for grain-boundary viscosity thus should equal that for grain-boundary diffusion, which is about 42 kJ/mole based either on assuming the activation energy for grain-boundary diffusion to be 2/3 the value for volume diffusion recommended by [16] or on the determination from measured grain-growth rates [17]. The agreement with our result is excellent.

Raj and Ashby [15] do not present any method for evaluating the boundary roughness,  $h$ , and few empirical studies exist. However, Schneibel and Petersen [18], in an excellent study on nickel at relative temperatures and stresses similar to those in firn, found that Equation (7) describes observations well and that  $h = 7\mu\text{m}$ . The best-fit viscosities calculated here yield  $h = 3\mu\text{m}$  for ridge BC,  $h = 4\mu\text{m}$  for site A and for South Pole, and  $h = 6\mu\text{m}$  for Dome C. This close agreement indicates that the viscosities calculated for ice by the model are physically reasonable.

It is evident from Figure 3 that the model does not predict the observed profile perfectly. In particular, the observed densification rate exceeds the modeled rate just below 2 m and again just above the critical point. At shallow depth the overburden pressure is small and other driving stresses, possibly arising from sintering of inhomogeneities [19], asymmetry of bonds [20], and slight temperature gradients may contribute to observed densification; with increasing depth these secondary driving stresses become insignificant compared to overburden pressure. Anisotropy also may play a role in shallow firn [9], and grain rotation as well as translation may have some effect on densification [20]. Near the critical point, our model may underestimate the contribution of other mechanisms to densification, and/or the model may terminate sliding densification too rapidly. Certainly, some grains maintain geometric freedom to slide after the point where the average grain loses such

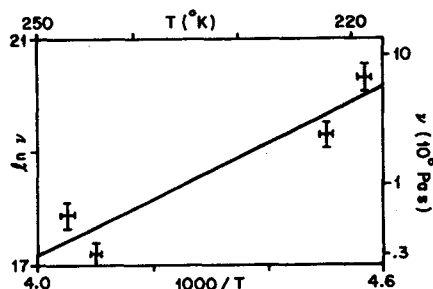


Fig. 4. Viscosity vs. temperature. The slope of the regression line gives the activation energy for viscosity.

freedom, so the termination of sliding is somewhat too abrupt in our model [21]. Also, it is possible that power-law-creep deformation does not reach steady state, so that faster, nonsteady creep parameters should be used to estimate densification by this mechanism. The possible effect of grain growth on densification also deserves further consideration [4].

Despite these difficulties, we believe that the model presented here provides a good first approximation of actual densification in highly porous polar firn. Densification occurs by Newtonian viscous sliding in response to overburden pressure; however, increase in density increases coordination number, which restricts the geometric freedom of grains to slide. Boundary sliding largely ceases as a primary mechanism of densification when the coordination number reaches 6 at a relative density of 0.6, and this causes the critical point in depth-density profiles. Although much work remains, a physically based model can predict depth-density profiles from measurements of temperature, accumulation rate, and the density, grain size, and bond size at 2 m depth.

Acknowledgements. I thank the Polar Ice Coring Office for core recovery, C.R. Bentley, J.H. Pereguzko, and I.M. Whillans for helpful comments, A.N. Mares and S.H. Smith for manuscript and figure preparation, and the National Science Foundation Division of Polar Programs for support through grants DPP-8315777 and DPP-8520846. This is contribution number 466 of the Geophysical and Polar Research Center, University of Wisconsin-Madison.

#### References

- [1] Gow, A.J., IAHS Publ. 114 (1975) 25-41.
- [2] Wilkinson, D.S., and Ashby, M.F., in Sintering and Catalysis, edited by G.C. Kuczynski (Plenum Press, New York) 1975, p. 473-492.
- [3] Maeno, N., and Ebinuma, T., J. Physical Chem. 87 (1983) 4103-4110.
- [4] Duval, P., Ann. Glaciology 6 (1985) 79-82.
- [5] Anderson, D.L. and Benson, C.S., in Ice and Snow, edited by W.D. Kingery (MIT Press, Cambridge, Mass.) 1963, p. 391-411.
- [6] Raj, R. and Ashby, M.F., Metallurgical Trans. 3 (1972) 1937-1942.
- [7] Hobbs, P.V., Ice Physics (Clarendon, Oxford) 1974, p. 258.
- [8] Alley, R.B., Bolzan, J.F. and Whillans, I.M., Ann. Glaciology 3 (1982) 7-11.
- [9] Alley, R.B., Ann. Glaciology 9 (in press).
- [10] Gotoh, K., and Finney, J.L., Nature 252 (1974) 202-205.
- [11] Gow, A.J., J. Glaciology 8 (1969) 241-252.
- [12] Coble, R.L., J. Appl. Phys. 41 (1970) 4798-4807.
- [13] Jaeger, J.C. and Cook, N.G.W., Fundamentals of Rock Mechanics, 3rd ed. (Chapman and Hall, London) 1979, p. 371-383.
- [14] Ashby, M.F., Surface Science 31 (1972) 498-542.
- [15] Raj, R. and Ashby, M.F., Metallurgical Trans. 2 (1971) 1113-1127.
- [16] Hobbs, P.V., Ice Physics (Clarendon, Oxford) 1974, p. 383.
- [17] Paterson, W.S.B., The Physics of Glaciers, 2nd ed. (Pergamon, Oxford) 1981, p. 18.
- [18] Schneibel, J.H. and Petersen, G.F., Acta Metallurgica 33 (1985) 437-442.
- [19] Evans, A.G., J. Amer. Ceramic Soc. 65 (1982) 497-501.
- [20] Petzow, G. and Exner, H.E., Z. Metallkunde 67 (1976) 611-618.
- [21] Ebinuma, T., and Maeno, N., J. Physique, this issue.

#### COMMENTS

C. HAMMER

The movement of vapor in the upper firn, due to barometric changes, will influence the grain size and shape. Your model uses spheres, which makes it difficult to include such an effect. What is your opinion on this ?

Answer :

There are important points, which I discuss only briefly in my manuscript. I assess the differences between the true geometry of firn and my present model in a separate paper (R.B. Alley, *Annals of Glaciology* 9, in press). The effects of vapor movement are strongest in the upper 2m, so I begin all calculations at 2m depth. I believe that the differences between modeled and observed depth-density curves between 2m and about 5-10m depth are caused by the geometric differences and vapor-transport effects that you mention.

---

Remark of J.R. PETIT :

The soluble impurity effect you suggest should be checked (empirically) by comparing growth rate of ice crystal observed in various coastal and inland polar sites, having a comparable mean temperature, but where soluble content (mainly of marine origin as sodium chloride) decreases as the distance from the coast increases. The distance effect between inland and coastal areas is of the same magnitude of the observed variation at Dome C between Holocene ice ( $\sim 20$  to  $40 \cdot 10^{-9} \text{ gg}^{-1}$  of Na) and Last Glacial ice ( $\sim 100$  to  $200 \cdot 10^{-9} \text{ gg}^{-1}$  of Na) respectively. From the available data, we conclude this effect possibly exist but remain small if compared to the "climatic effect" we suggest as the first governing parameter (Petit et al., this symposium).

But, an important problem is always unsolved. What impurities can be dissolved in the lattice? And what is the physical mechanism for grain boundary migration?

Answer :

I agree that it is of critical importance to know the concentrations of dissolved impurities rather than of soluble impurities; if the sea salt and volcanic acids are present as microparticles they will have little effect on grain growth, but if these same impurities dissolve in the ice we expect a large effect. It is quite possible that the fraction of soluble impurities that actually dissolves varies. A demonstration that the dissolved impurity concentration does not affect growth rate would invalidate our theory, of course, but I do not believe that the available data do so. I still consider our explanation of small grain sizes in Wisconsinan ice at Dome C to be most likely (though certainly not proven) because it seems more probable physically, but I am intrigued by your theory and wish to study it more carefully. It also is important to remember that the grain-growth rate is an exponential function of temperature but only a linear function of dissolved impurity content in our theory, so that small errors in temperature determination may obscure some impurity effects in comparisons between sites.

---

T.H. JACKA

Sharp crystal size changes have been associated with high shear zones at some Antarctic ice core sites.

In addition, recent ice deformation tests have resulted in the development of equilibrium crystal sizes. Could you comment on the possible effect of shear on crystal sizes found in Polar ice cores.

Answer :

At depths where shear deformation is significant, it clearly has greater effect on grain size than any of the considerations discussed here, as you have shown in your work (e.g. Jacka and Qun, this conference). There probably is a strong interaction between deformation and the effects discussed here, however. For example, Gow and Williamson (CRREL Report 76-35, 1976) describe volcanic-ash-rich layers from the Byrd Station core that have small grain sizes and strong c-axis fabrics compared to

adjacent, clean ice, and show that these are regions where shear deformation is localized. Our calculations show that the concentrations of microparticles and impurities in these layers are large enough to reduce grain-growth rates significantly. We expect that the small grain sizes arising from the particle and impurity effects, and/or these materials themselves, soften the ice and localize deformation, which further reduces grain size.

---

N. MAENO

Do you have any evidence supporting that you need not take into account the possible densification in the horizontal plane ?

Answer :

In most firn the horizontal area occupied by a bulk sample does not change during sintering, so all densification must occur by vertical strain. This raises the important question of the horizontal stress state, however. I have assumed that each grain experiences a vertical force that causes downward motion relative to its neighbors, and I note in the manuscript that this is a reasonable assumption to make. However, it is certain that horizontal forces are important on at least some grains, and a more-complete model would include this. I believe that field measurements of the horizontal stress state in firn are needed before such a complete model can be constructed.

---

J.W.GLEN

Do you mean impurities in the lattice or impurities in the grain boundary. I would expect impurities in the grain boundaries to be far the most important in affected grain boundary movement.

Answer :

The drag on grain-boundary migration is caused by impurities in the grain boundaries. The grain-boundary impurity concentration is related to the lattice impurity concentration by the fractionation factor which may be about  $10^3$  for NaCl in ice. J.W. Cahn (1962, Acta Metallurgica, 10, 789) formulated his impurity-drag theory in terms of the lattice concentration, and we have continued to use this formulation but it is easily converted to a boundary concentration.

---

C. HAMMER

Remark :

John Glen just raised the question, if the impurities are dissolved in the grains. I made experiments on high impurity ice from Greenland ice cores, which shows that the impurities are indeed in the grains. Grain boundaries can show very high concentrations, but they only contain a small fraction of the total amount of impurities in an ice sample.

(see eg. Hammer and Clausen, This conference)

Answer :

I agree completely. In our papers on this subject (R.B. Alley, J.H. Pereguzko and C.R. Bentley, in press, a, b, Journal of Glaciology) we show that if grain-boundary impurity concentrations in cold ice are  $\sim 10^4$  lattice impurity concentrations, then almost 100% of the impurities are contained in the lattice because the total volume of highly impure boundary is insignificant.